Journal of the Korean Geographical Society, Vol. 44, No. 2, 2009(105-121)

Estimating Air Temperature over Mountainous Terrain by Combining Hypertemporal Satellite LST Data and Multivariate Geostatistical Methods

Sunyurp Park*

초단주기 지표온도 위성자료와 다변량 공간통계기법을 결합한 산지 지역의 기온 분포 추정

박선엽*

Abstract : The accurate official map of air temperature does not exist for the Hawaiian Islands due to the limited number of weather stations on the rugged volcanic landscape. To alleviate the major problem of temperature mapping, satellite-measured land surface temperature (LST) data were used as an additional source of sample points. The Moderate Resolution Imaging Spectroradiometer (MODIS) system provides hypertemperal LST data, and LST pixel values that were frequently observed (≥14 days during a 32-day composite period) had a strong, consistent correlation with air temperature. Systematic grid points with a spacing of 5km, 10km, and 20km were generated, and LST-derived air temperature estimates were extracted for each of the grid points and used as input to inverse distance weighted (IDW) and cokriging methods. Combining temperature data and digital elevation model (DEM), cokriging significantly improved interpolation accuracy compared to IDW. Although a cokriging method is useful when a primary variable is cross-correlated with elevation, interpolation accuracy was sensitively influenced by the seasonal variations of weather conditions. Since the spatial variations of local air temperature are more variable in the wet season than in the dry season, prediction errors were larger during the wet season than the dry season.
Key Words : Hawaiian Islands, MODIS LST, IDW, cokriging, interpolation

요약 : 지형 굴곡이 심한 하와이 화산섬의 경우, 측후소 분포가 매우 제한적이어서 공식적인 기온 분포도가 작성되지 못하고 있는 실정이다. 본 연구에서는 이러한 기온 지도화의 문제점을 해결하는 방법으로 위성기반의 지표온도 자료로부터 기온추정치를 추출하여 내삽법에 필요한 입력자료로 사용하였다. 추출된 온도값을 표본값으로하여 거리 역비례 가중치법 (IDW)과 공동크리깅 (cokriging)을 적용하여 기온추정치를 지도화하였다. 기온과 고도값을 함께 이용한 cokriging이 IDW에 비해 크게 향상된 추정 오차값을 나타내었다. Cokriging은 주 변수와 고도와 같은 추가 변수 간의 상관관계가 유의하게 나타날 때 효과적으로 사용되는 내삽법이지만, 내삽 정확도는 계절적인 기상조건에 민감하게 영향받는 것으로 조사되었다. 강수량이 크게 증가하는 우기에는 건기에 비해 공간적인 기온변화가 크며, 이에 따라 기온 추정 오차값도 우기에 높게 나타났다.
주요어 : 하와이, 지표온도, 거리 역비례 가중치법, 공동크리깅, 내삽법

* Assistant professor, Department of Geography and Environmental Studies, University of Hawaii-Hilo, sunypark@hawaii.edu

1. Introduction

Continuous air temperature and precipitation data are important variables in a wide range of environmental applications. The usage of these basic meteorological inputs is highly limited due to lack of data in mountainous areas. In rugged volcanic environments, in particular, the networks of weather stations are not dense enough to accurately estimate the meteorological parameters using interpolation methods. In addition, precipitation and air temperature constantly change with elevation, and this phenomenon, known as the orographic effect, is commonly observed on volcanic mountain slopes. Moreover, relationships between the variables and elevation may change over time and space. For example, precipitation increases and air temperature decreases continuously with increasing elevation in midlatitude regions (Lull and Ellison, 1950; Barry and Chorley, 1987). However, maximum precipitation and temperature inversions occur below mountain tops in tropical and subtropical regions (Giambelluca and Nullet, 1991; Daly *et al.*, 1994; Nullet *et al.*, 1995). As a result, the horizontal and vertical variations of the climatological variables may not be represented by data collected from the sparse networks of weather stations.

In the Hawaiian Islands, meteorological data are limited in both temporal and spatial dimensions. Weather stations are not evenly distributed, but they are often located in densely populated coastal areas. Especially, air temperature data, such as daily and monthly air temperature, are not recorded at all weather stations, and they are commonly missing due to severe weather conditions and malfunction or lack of maintenance of meteorological devices. Therefore, temporally continuous data are available from only a small number of weather stations. For instance, daily air temperature data of 2007 are available only from thirteen weather stations in the Island of Hawaii, the biggest island of Hawaii, with the density of one weather station per 802.5km^2.

Spatial and temporal continuity of air temperature data can be enhanced by satellite-measured surface temperature data. Although satellite-based land surface temperature (LST) data are only available under clear sky conditions, broad geographic coverage of satellite systems with a hypertemporal resolution may provide an opportunity for researchers to produce air temperature maps with improved quality. One of the most commonly used hypertemperal LST data sources is the Moderate Resolution Imaging Spectroradiometer (MODIS) system. MODIS provides daily satellite coverage of a variety of wavelength bands, and its data products are designed to provide consistent monitoring of earth with various spatial resolutions (Justice *et al.*, 1998; Kaufman *et al.*, 1998). Considering its high radiometric resolution (12 bits) and calibration accuracy in multiple thermal infrared bands, MODIS is useful for LST detection (Barnes *et al.*, 1998; Kaufman *et al.*, 1998). Corrected for atmospheric effects, the MODIS system provides daytime and nighttime LST data for scientific applications along with additional layers of quality assessment, clear sky coverage, and observation times. If regularly-sampled LST data represent air temperature well, they may be used as additional control points for more accurate spatial interpolation of air temperature. This study investigated the potential usage of MODIS LST data in spatial interpolation to improve the accuracy of the air temperature map of a mountainous island using cokriging.

2. IDW and cokriging

Interpolation is a common surface modeling process for continuous phenomena that are surveyed or measured at a limited number of sampling locations. Inverse distance weighted (IDW) interpolation is the most commonly used method. Assuming the spatial dependence of point values, known as the spatial autocorrelation, the estimated value of a location is more heavily influenced by closer known values than those farther away. IDW works reasonably well as long as known values, or control points, are distributed with a pseudoregular pattern, but it has major limitations if the number of control points is very small and sparsely gridded. Since the method is only based on distances between points to be estimated and known points, local peaks and valleys of a surface that the method predicts may not be accurately represented unless a fine network of control points exists. Considering the importance of the number of control points for preservation of local influence, researchers reported that a smaller number of control points were better than a larger number (Zimmerman *et al.*, 1999).

Kriging methods, in general, are also based on spatial dependence. It is a generalized least-square regression technique that allows an analyzer to account for the spatial dependence between known points (Goovaerts, 2000). In kriging, spatial autocorrelation is computed as semivariance, and it is plotted against distance in a semivariogram for optimal predictions. The semivariance is computed by:

$$\gamma(h)=\frac{1}{2}[z(x_i)-z(x_j)]^2$$

where $\gamma(h)$ is the semivariance between two known point values, $z(x_i)$ and $z(x_j)$, with a distance of h. Normally, a semivariogram cloud consisting of all pairs of known points is divided into a manageable number of lags, a process called binning. If sampling points are located on a pseudoregular grid, their grid spacing is usually a good lag size (Isaaks and Srivastava, 1989). Once a lag size is decided, mean semivariance is computed for each lag interval:

$$\gamma(h)=\frac{1}{2n}\sum_{i=1}^{n}[z(x_i)-z(x_i-h)]^2$$

where $\gamma(h)$ is the mean semivariance between two known points, $z(x_i)$ and $z(x_j)$, with a lag distance of h, and n is the number of known points in each interval. As a result, a semivariogram represents mean semivariance values against distance intervals an analyst chooses. To use a spatial relationship between points in kriging, the semivariogram needs to be fitted with a mathematical model. Three common models include spherical, exponential, and Gaussian. A spherical model shows a gradual decrease of spatial dependence of a variable as a distance between two points increases. An exponential model applies when the spatial dependence decreases exponentially with increasing distance and disappears completely at an infinite distance. In a Gaussian model, the spatial dependence also vanishes at an infinite distance. The unique feature of this model is its parabolic shape at the origin.

In mountainous areas, elevation is commonly used as secondary input data to interpolation if a primary variable is spatially correlated with it (Martinez-Cob and Cuenca, 1992; Phillips *et al.*, 1992; Daly *et al.*, 1994; Martinez-Cob, 1996; Daly *et al.*, 2003). A secondary variable is often useful in an interpolation process if the primary variable is undersampled (Issaks and Srivastava, 1989; Goovaerts, 2000). Cokriging is a multivariate approach of kriging and uses one or more

additional variables to estimate a primary variable of interest. Hevesi *et al.* (1992) used cokriging to estimate mountainous precipitation and found that cokriging reduced estimation variances by 55% relative to univariate kirging. In a volcanic-island setting, temperature is strongly correlated with elevation, and a correlation between the two variables can be used in cokriging to reduce the prediction errors of temperature estimation. A cokriging estimate is a linear combination of both primary and secondary variables and is given by (Issaks and Srivastava, 1989):

$$u_o = \sum_{i=1}^{n} a_i * u_i + \sum_{j=1}^{m} b_j * v_j$$

where u_o is the estimate of U, the primary variable, at location o; $u_1 \ldots u_n$ are the primary known values at nearby locations 1 through n; $v_1 \ldots v_m$ are the secondary known values at nearby locations 1 through m; a_i and b_j are cokriging weights.

Although kriging is more advanced and complex than IDW, a preliminary experiment showed that univariate kriging did not outperform IDW in the study area. As Declercq (1996) indicated, the most important factors in interpolation may include the number of control points and the nature (or type) of a phenomenon under investigation rather than interpolation methods themselves. To evaluate how much a multivariate kriging method improves interpolation results compared to a univariate method, IDW and cokriging methods were compared in this study. Considering temperature changes on the radial terrain that is characterized by two large shield volcanoes, the existence of a spatial trend, or a drift of air temperature is not assumed. Therefore, an ordinary cokriging approach was used in the analysis.

3. Methods and materials

1) Study area

The seven main islands of Hawaii were selected for the study (Figure 1). While the Hawaiian Islands are constantly influenced by the year-round northeasterly trade winds, the microclimates of the region rapidly change across

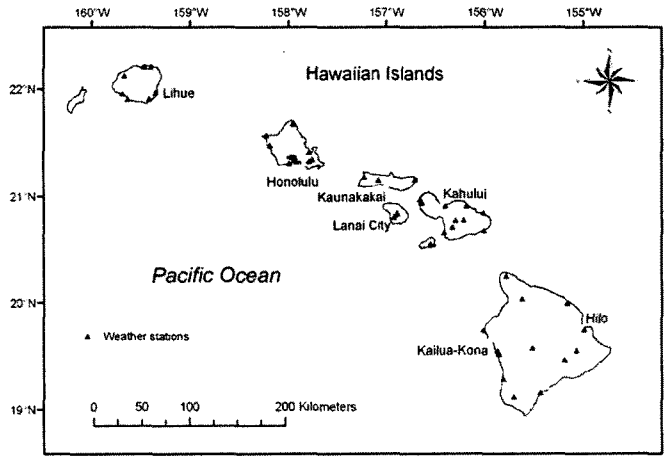

Figure 1. Study area

The locations of statewide forty four weather stations and major cities are shown on the map.

the landscape depending on slope aspect, elevation, topography, and frequency of storms. The orographic effect of volcanic mountains creates a dramatic precipitation contrast between the east and west slopes of the islands. As a result, precipitation ranges from less than 200 mm/yr on the leeward side (west) to more than 7,000 mm/yr on the windward side (east) of the Island of Hawaii, the largest island in Hawaii (Nullet *et al.*, 1995). Hawaii has the typical seasonal cycles of rainfall with the cool, wet season (October-April) and the warm, dry season (May-September), and the seasonality is strongly controlled by the pattern of the trade winds and the frequency of storm development.

The seasonal temperature variations of the Hawaiian Islands are small due to their maritime environment. Annual temperature variations are typically less than 5°C, and annual temperature ranges from 23°C to 24°C for most coastal areas. However, vertical temperature gradients are significant, and annual mean temperatures at high elevation are much colder than lowlands. For example, the summits of two main mountain systems in the Island of Hawaii, Mauna Loa and Mauna Kea, are higher than 4,100 meters above the mean sea level and have mean annual temperatures of lower than 6°C (Nullet and Sanderson, 1995). Volcanic activities, which created the progressively varying ages of Hawaiian Islands, dramatic climatic contrasts, and undulating surface terrain contributed to the uniqueness of Hawaiian plant compositions. The dynamic physical system of the Hawaiian environment supports one of the most complex ecological diversities in the world (Vitousek *et al.*, 1992).

2) Satellite data

MODIS LST 8-day composite products (MOD11A2) were downloaded from the EROS Data Center for 2007 (https://wist.echo.nasa.gov). Two image tiles (03/06 and 03/07) were mosaicked together to cover the main Hawaiian Islands. LST data were missing for two composite periods (02/18/2007-02/25/2007 and 03/06/2007-03/13/2007). Therefore, forty four total LST 8-day composite images were processed. Each 8-day composite includes the mean LST of the composite days excluding cloud-contaminated days for both daytime (data acquisition time = approximately 10-11am) and nighttime (data acquisition time = approximately 10-11pm). Each data composite also includes ancillary information, indicating which days were under clear sky and used for calculation of the mean LST. Therefore, the days and number of days that were observed by the satellite system were determined for each composite period. Finally, four consecutive 8-day composites were averaged to create twelve 32-day composite images.

Since LST is influenced by the varying conditions of the surface, determination of a relationship between LST and air temperature requires close examination of data acquisition days and times at data collection points for both satellite- and ground-based temperature data. Correlation analysis was performed for both daytime and nighttime LST data, and the number of observations of each 32-day LST composite was used as a parameter for selection of LST pixels. It was hypothesized that a mean LST pixel value computed from more frequent observations would better represent the mean air temperature of that pixel for each composite than that computed from a fewer number of observations. To select sample points from LST composites, regularly spaced points were generated using the Hawth's Analysis Tools, an ArcGIS extension for spatial analysis and functions (freely available from http://www.spatialecology.com/htools/). Three different spacings were selected: 5km, 10km, and 20km (Figure 2). After these grid

layers were generated, a LST value for each grid point was extracted from each LST composite for further analyses.

3) Air temperature data

Daily air temperature data of 2007 were downloaded from National Climate Data Center (http://www.ncdc.noaa.gov). The data were available from 44 weather stations of the National Weather Service (NWS)'s Cooperative Station Network across the islands. However, daily records were not continuously collected at all weather stations. The number of weather stations that held daily records for more than 300 days was only 27 stations (61.4%). 13 weather stations (29.6%) had daily records for more than 200 days (but less than 300 days), and 4 weather stations held daily records for less than 200 days. These daily air temperature data were integrated into twelve periods using the same 32-day composite periods of the LST data. After the 32-day mean air temperature data were prepared for the 12 composite periods, a linear relationship between the air temperature and LST of all composite periods at the 44 weather station locations was determined.

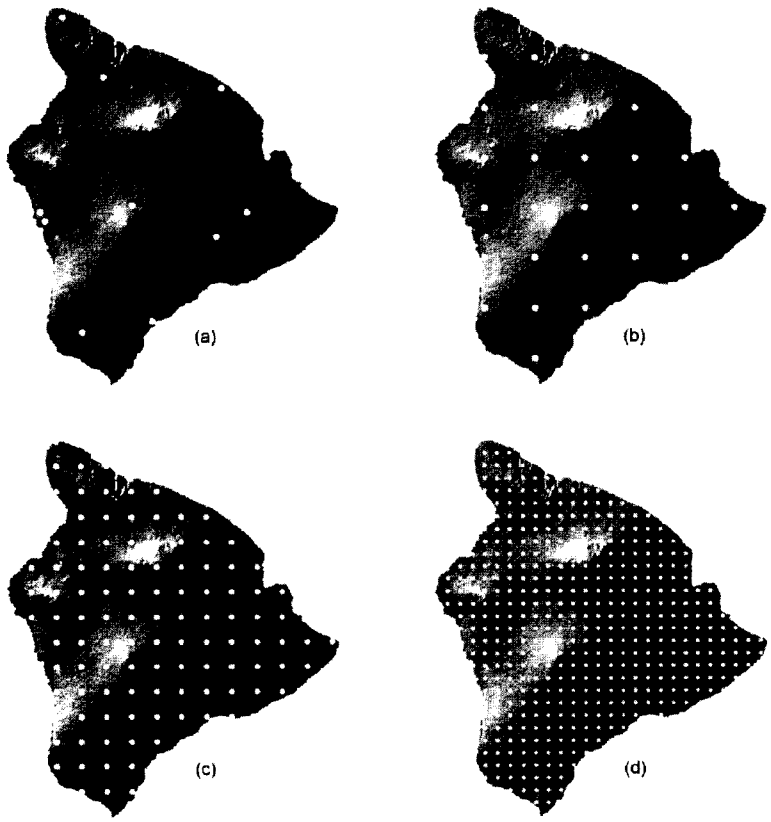

Figure 2. The National Weather Service' s Cooperative Station Network in the Island of Hawaii (a) and three sample-point grids with a distance of 20km (b), 10km (c), and 5km (d)

The hill-shading image of the surface terrain of the island is also provided on the background.

4) Interpolation parameters

The Island of Hawaii was selected for interpolation experiments considering its land size and large gradient of elevation. Using the Geostatistical Analyst extension of ESRI ArcGIS 9.3, IDW and cokriging methods were applied to the air temperature data of the weather stations and the LST-derived air temperature estimates of sampling grid points with three different spacings (5km, 10km, and 20km). Assuming that there was no surface trend in the data other than the influence of elevation, an ordinary cokriging approach was selected. Thirteen weather stations are located in the island, and 312, 91, and 35 additional LST sample points were selected from the 5km, 10km, and 20km grid points. However, only a certain number of LST-derived air temperature estimates were included in interpolation depending on the number of LST observations for each composite. To determine the number of pixel observations that made the LST-estimated air temperature statistically representative of air temperature, a correlation analysis was conducted. After this pixel selection process, the two interpolation methods were applied to four separate data sets:

1. Weather station data only (13 weather stations)
2. Weather station data + LST-derived temperature data from 20km grid points
3. Weather station data + LST-derived temperature data from 10km grid points
4. Weather station data + LST-derived temperature data from 5km grid points

Spatial dependence decreases as a distance between two locations increases, and sample points beyond a certain distance will have little or no correlation with a point value to be estimated. Therefore, it is common practice to select directional configuration and the number of control points that will be used in the prediction of an unknown value. No directional difference in spatial dependence was assumed, and an isotrophic model was used. For sample-point selection, simple and quadrant strategies were used for all data sets (Slocum *et al.*, 2009). For the simple strategy, no direction was specified, and 8 control points or the minimum of 4 points that fell within a search circle were used for both interpolation methods. For the quadrant strategy, 4 control points or the minimum of 2 sample points that fell within each of the four cardinal sectors of a search circle were used.

Selection of a fitting model to a semivariogram is an important task in kriging. Previous studies reported that data characteristics, visual inspection, and cross-validation were important in a model-selection process (Webster and Oliver, 2001; Jarvis *et al.*, 2003). In this study, the semivariogram of each composite data was fitted with two conceptually plausible models, spherical and Gaussian, to determine an optimal model for the island setting. Considering the strong correlation between elevation and air temperature, erratic changes of air temperature over short distance were not expected to exist, and spatial dependence was assumed to decrease progressively with increasing distance. For lag size, 10km was used for the data set 1, while the intervals of grid points (5km, 10km, and 20km) were used for the other data sets. The result of this parameterization was evaluated by cross-validation.

USGS Digital Elevation Model (DEM) was used as a secondary input variable to cokriging. A 30-meter resolution DEM was downloaded from the National Elevation Dataset (NED) website (http://ned.usgs.gov/), and resampled to 100 meters. The annual mean air temperature has a strong, inverse relationship with elevation (r^2 = 0.93, $P < 0.0001$). Based on data from statewide weather stations, the environmental lapse rate was determined as 6.0°C/km.

5) Cross-validation

Although the distinct spatial pattern and visual appearance of a phenomenon of interest are an important means of evaluation of an interpolation method, cross-validation is commonly performed to numerically check for the accuracy of the interpolation method. Cross-validation evaluates the accuracy of interpolation by removing a known point from the data set, interpolating the value at that point with the remaining control points, and calculating a difference between the predicted value and the known value. After repeating the process for all known points, the mean prediction error is determined as a diagnostic statistic, known as the root mean square error (RMSE):

$$RMSE=\sqrt{\frac{1}{n}\sum_{i=1}^{n}(z_{io}-z_{ie})^2}$$

where n is the number of points, z_{io} is the known value of point i, and z_{ie} is the estimated value of point i. Another statistic that is routinely computed for cross-validation is root mean square standardized error (RMSSE):

$$RMSSE=\sqrt{\frac{1}{n}\sum_{i=1}^{n}\frac{(z_{io}-z_{ie})^2}{s_i^2}}=\frac{RMSE}{s}$$

where s_i is the estimated prediction standard error of point i and s is the mean prediction standard error. This statistic provides the assessment of uncertainty of predictions by estimating the variability of the predictions from known values. If the mean of prediction standard errors is close to RMSE, the interpolation method is correctly assessing the variability of the predictions. If the mean of prediction standard errors is greater than RMSE (that is, RMSSE < 1), the interpolation method is overestimating the variability of the predictions. If the mean of prediction standard errors is less than RMSE, RMSSE becomes greater than 1 and the interpolation method is underestimating the variability of the predictions.

4. Results and discussion

1) Selection of LST data for interpolation

Daytime and nighttime LST data were compared to mean, maximum, and minimum air temperatures collected at the weather stations. A relationship between air temperature and LST was severely distorted during the day due to strong heat fluxes to the surface. As a result, daytime LST did not show a significant correlation with elevation (Figure 3). However, nighttime LST had a strong, linear inverse relationship with elevation (r^2=0.93), and showed the same lapse rate as that of ground-measured air temperature (6.0°C/km). A comparison between 32-day LST composite data and air temperature showed that nighttime LST was statistically representative of 32-day mean, maximum, and minimum air

Table 1. Correlations between LST and air temperature (mean, maximum, and minimum)

	LST_day	LST_night	LST_mean
Mean_air	0.27	0.96	0.79
Significance*	0.01	0.01	0.01
n †	222	205	129
Max_air	0.33	0.94	0.81
Significance	0.01	0.01	0.01
n	222	205	129
Min_air	0.21	0.94	0.75
Significance	0.01	0.01	0.01
n	222	205	129

* The level of significance (α) of Pearson's correlation coefficients.

† Number of observations.

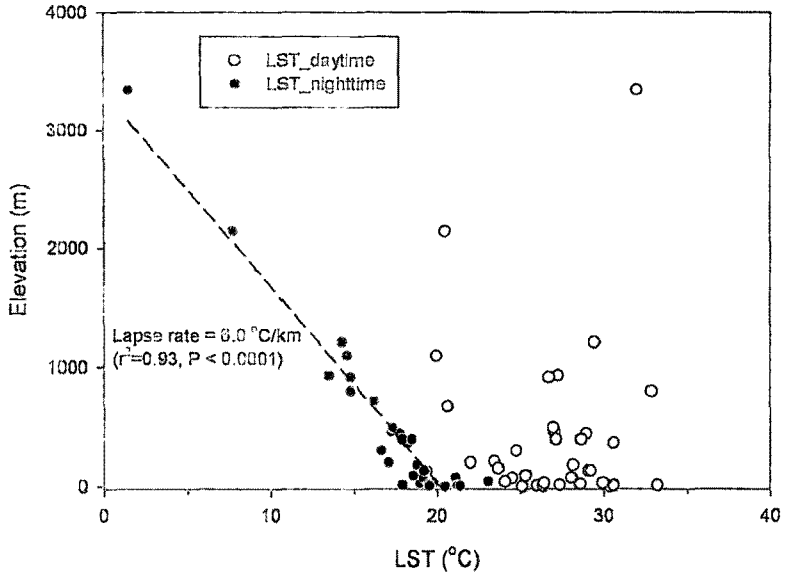

Figure 3. A relationship between MODIS LST data and elevation

The nighttime LST decreases as elevation increases with the same lapse rate as that of air temperature. However, the daytime LST did not have any significant relationship with elevation.

temperatures (Table 1).

The number of LST observations at each pixel during a composite period was an important criterion in selecting a LST value most representative of air temperature. A correlation between LST and air temperature increased as the number of LST observations increased. The relationship leveled off as the number of pixel observations reached 14 days, and its correlation coefficient became greater than 0.95 (Figure 4a). Therefore, only those LST pixels that were acquired for at least 14 days were considered as input data to interpolation. With this condition, a linear relationship between LST and air temperature(Figure 4b) was computed as:

Air temperature (°C)=5.2517+0.9411 × LST

Annually, the number of clear-sky days was very low on windward slopes while it was higher on leeward slopes and dry highland of the island. Therefore, the density of sample points tends to be lower in cloud-prone eastern areas than in dry western and highland areas.

2) Impact of seasonality on prediction errors

Strong climatic seasonality intensifies the unevenness of rainfall distribution and temperature variations in the Hawaiian Islands. The trade winds dominate in the warm season, and they make the local weather stable and dry. In the cool season, however, they weaken, and local weather is characterized by variable, humid winds and heavy rain (Schroeder, 1995). The temperature inversion occurs more frequently in the warm season than the cool season due to the stronger subsidence of the Hadley Cell. As a result, an averaged environmental lapse rate (ELR) and the spatial variations of air temperature increased in the cool season (Figure 5).

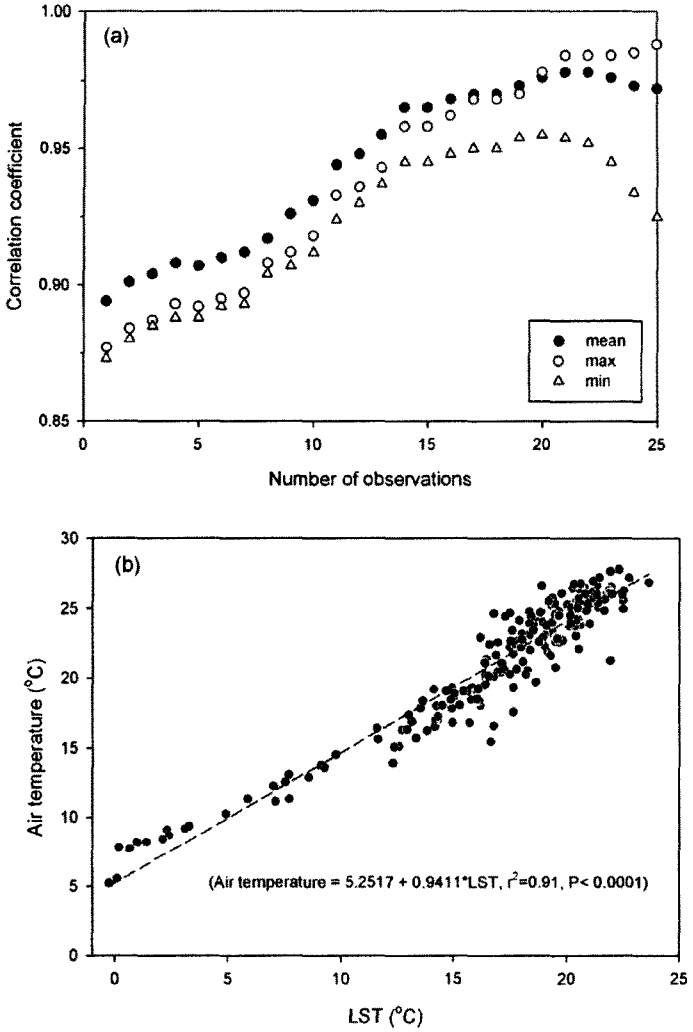

Figure 4. Correlation coefficients between nighttime-LST and air temperature as a function of the number of LST observations per composite period (a), and a linear regression model that is established based on and LST pixel values acquired for at least 14 days during each composite period and the mean air temperature computed for the same composite period (b).

The nighttime LST data have the strongest correlation with the mean air temperature. The correlation coefficients increase until the number of the LST observations reaches 14 days, but it levels off after that.

Regardless of interpolation methods and models, prediction errors measured by RMSE increased with the increasing standard deviation of air temperature (Figure 6). Since ELR and the spatial variations of temperature increased in winter months, the accuracy of interpolation tended to decrease in the cool, wet season. Figure 7 shows that the RMSE scores of the three interpolation methods were low in the warm season and high in the cool season. Although cokriging is based on an observed cross-correlation between the primary and secondary variables, a stronger correlation between the two variables in the cool season does not necessarily

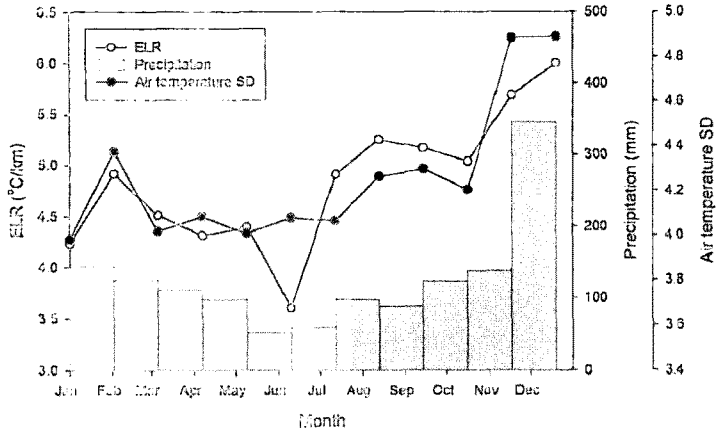

Figure 5. Environmental lapse rates (ELR) are computed for each composite period and plotted along with rainfall data and the standard deviation (SD) of air temperature

Precipitation increases in winter (the cool, wet season), and ELR and the variance of air temperature also increase in a similar pattern. For each composite period, weather stations that are missing rainfall data for more than 3 days (or more than 10%) are ignored. Also, the total rainfall of the last composite period (12/19/2007-12/31/2007) is not shown because it consists of only 13 days.

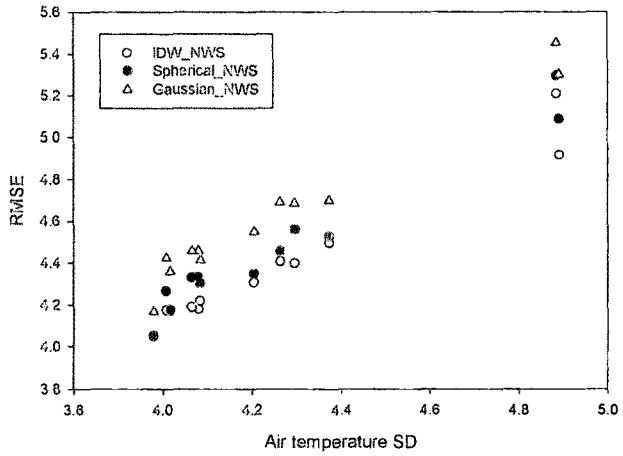

Figure 6. Relationships between the prediction errors (RMSE) of the three interpolation methods and the standard deviations (SD) of air temperature collected at the thirteen weather stations of the National Weather Service's Cooperative Station Network in the Island of Hawaii

The spatial variations of air temperature have a direct relationship with prediction errors.

improve interpolation accuracy.

A correlation between air temperature and elevation is typically higher in the cool season than in the warm season as ELR increases in the cool season. However, local weather is more variable in the cool season, and it causes higher prediction errors of interpolation. A recent study conducted on a volcanic island (Jeju Island, Korea) showed that the performance of a cokriging method was directly related to a correlation between air temperature and elevation (Park and Jang, 2008). However, it is not safe to

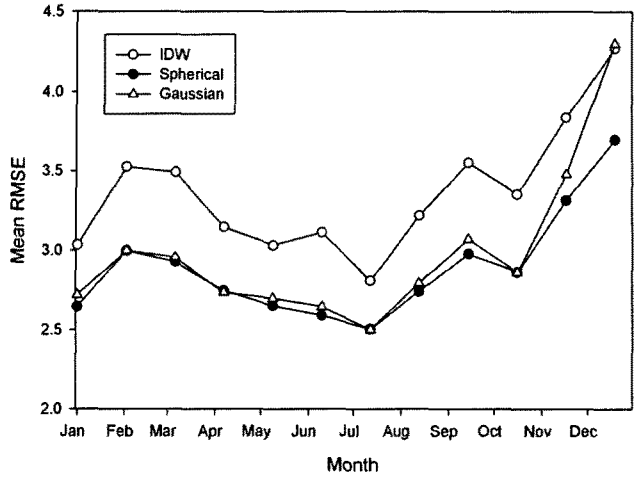

Figure 7. The seasonal variations of mean RMSE' s computed by each interpolation method

RMSE scores based on the four sample point densities (NWS' 13 weather stations, 20km, 10km, and 5km grids) are averaged. RMSE scores are lower in the warm, dry season (summer months) than in the cool, wet season (winter months).

confirm the relationship knowing that they used meteorological data for only four months (January, April, August, and October) and lacked seasonal analyses of vertical variations of air temperature in the island whose peak is lower than 2,000m. Ishida and Kawashima (1993) reported that strong radiation balances due to daytime heating and nighttime cooling might have caused the short-distance variations of air temperature and higher prediction errors of cokriging in summer and winter. Their study indicated that local environments could sensitively influence the accuracy of spatial prediction. It should be noted, therefore, that both a cross-correlation among variables and the spatial variability of a primary variable contribute to the quality of interpolation products.

3) Interpolation models and parameters

Air temperature data were available only from thirteen weather stations of the Island of Hawaii. With the limited number of sample points, interpolation maps produced by IDW and cokriging methods had similar RMSE scores ranging from 4.46 to 4.50 (Table 2). In other words, the DEM data as a secondary variable in cokriging did not improve the accuracy of the interpolation. The spacing of sample points had a linear inverse relationship with the prediction errors of the cokriging methods (Figure 8). The relationship shows that prediction errors decreased when the MODIS LST-derived 20km-grid samples were combined with the NWS' temperature records as input data. But, there was no significant difference in prediction errors between IDW (RMSE=3.65) and the two cokriging (RMSE=3.38 and 3.60) models. When the two finest grids, which have a spacing of 10km and 5km, were used as input, the cokriging models outperformed the IDW method significantly. For example, the mean prediction error of the Gaussian model was smaller than that of IDW by 31% for the 10km grids and by 33.6% for the 5km grids.

With these fine densities of sample points, the prediction errors of the two cokriging models were not significantly different from each other.

Table 2. The annual mean of RMSE, ASE, and RMSSE computed from IDW and spherical and Gaussian models of cokriging

Search strategy		Simple			Quadrant		
Grid	Score	IDW	Spherical	Gaussian	IDW	Spherical	Gaussian
Cooperative (N=13)	RMSE	4.46	4.89	4.90	4.39	4.48	4.64
	ASE	-	4.13	4.24	-	4.09	4.18
	RMSSE	-	1.07	1.11	-	1.00	1.08
20km (N=25.2)	RMSE	3.58	3.47	3.60	3.65	3.38	3.60
	ASE	-	4.68	4.59	-	4.66	4.57
	RMSSE	-	0.72	0.86	-	0.71	0.87
10km (N=56.7)	RMSE	3.42	2.52	2.49	3.40	2.39	2.35
	ASE	-	3.80	3.51	-	3.77	3.44
	RMSSE	-	0.70	0.77	-	0.68	0.74
5km (N=182.8)	RMSE	2.09	1.44	1.37	2.02	1.30	1.34
	ASE	-	2.46	2.01	-	2.43	1.97
	RMSSE	-	0.54	0.67	-	0.51	0.65
Mean	RMSE	3.39	2.98	2.99	3.38	2.89	2.94
	ASE	-	3.87	3.66	-	3.84	3.63
	RMSSE	-	0.74	0.82	-	0.72	0.81

Two different strategies of sample point selection, simple and quadrant, were employed. The total number of sample points (N) used in interpolation is averaged over the twelve composite periods.

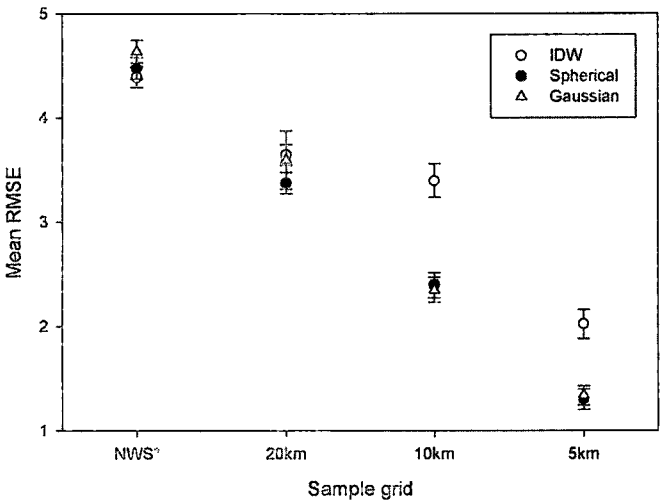

Figure 8. The annual mean of RMSE scores computed by IDW and cokriging based on two models fitted to semivariogram: spherical and Gaussian

RMSE scores decrease linearly as the spacing of sample points decreases. Whiskers above and below each symbol represent the standard errors of RMSE at sample points. Distance between two adjacent NWS weather stations varies significantly, ranging from 4.0km to 28.6km. The averaged standard deviation of distances between two nearest weather stations is 26.8km.

However, the Gaussian model produced a more reliable result compared to the spherical model. The average standard error (ASE) of the Gaussian model was 24.8% and 37.2% smaller than that of the spherical model for the 10km and 5km grid data sets. This result reveals that the elevation-dependent changes of air temperature causes the gradual change of the semivariance of the primary variable.

The spatial patterns of interpolation maps created by IDW and cokriging methods were compared to each other using January and July temperatures (Figure 9). Overall temperature patterns agreed to each other, representing low temperatures at four major volcanic mountain peaks of the island. However, IDW failed to represent coastal temperature patterns that are typically parallel to the coastlines. The IDW method frequently produced rugged isotherms, and did not provide an intimate relationship between air temperature and elevation. Combining temperature data with elevation information, cokriging represented progressive temperature changes with elevation. Smooth isotherms are well represented for dry highlands and leeward slopes (western slopes), but their smoothness was reduced on the wet, windward slopes (eastern slopes), where the density of satellite-derived sample points was lower than the dry slopes due to cloudy conditions. Since annual

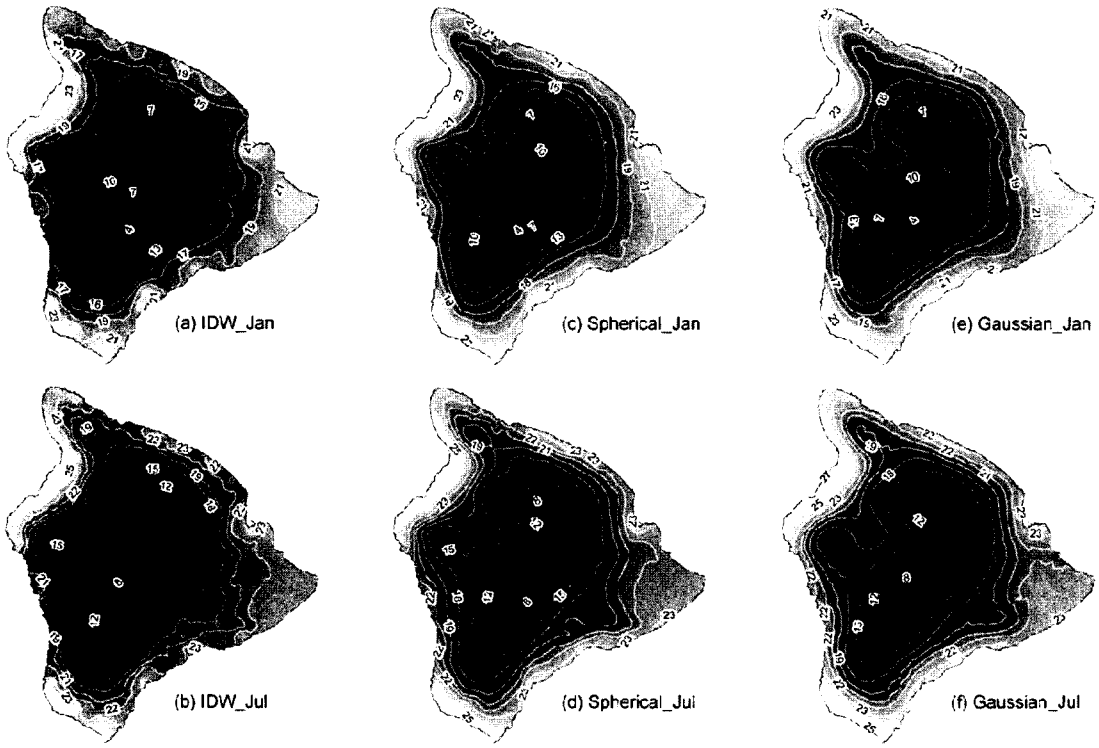

Figure 9. Comparison of IDW and two cokriging methods using 5km-grid data of January and July 2007

Maps (a), (c), and (e) show interpolation results from IDW and the two cokriging methods (spherical and Gaussian models) for January. Maps (b), (d), and (f) show the same results for July. The prediction errors (RMSE) of the January map are 1.66, 1.01, and 1.05 for IDW and the spherical and Gaussian models. The prediction errors of the July map are 1.39, 0.89, and 0.97 for the same methods. Unit =°C.

temperature ranges are small on the tropical island, there was little change in temperature patterns between January and July.

The two different sample-point selection strategies produced similar prediction results, but the quadrant strategy produced lower RMSE and ASE scores than the simple strategy for all interpolation methods. This means that prediction errors and the variance of estimation can be reduced if sample points are selected from various directions. Therefore, four cardinal directions should be considered for sample-point selection on the volcanic mountainous terrain.

5. Conclusions

Temperature estimation on volcanic terrain is a challenging task. The limited number of weather stations is the primary source of inaccurate predictions in an interpolation process. The low spatial density of weather stations was alleviated in this study by sampling satellite LST data at regularly-spaced grid points. Study results showed that 32-day mean LST composites had a constant, strong correlation with air temperature as long as LST observations were acquired for 14 days or more frequently during each composite period. In addition to the increased number of sample points, a strong inverse relationship between air temperature and elevation was used to further reduce prediction errors. Cokriging, a multivariate geostatistical method, incorporated both temperature samples and elevation into the interpolation process and generated a temperature map that was more accurate than an IDW-based map. Considering the gradual change of air temperature over surface terrain, it is believed that the Gaussian model is more dependable than the spherical model in cokriging. The Gaussian model describes a spatially continuous random function (or a variable to be estimated), while the spherical model describes a less continuous phenomenon (Issaks and Srivastava, 1989). An experiment conducted in the study showed that the Gaussian model produced the average standard error (ASE) of estimation significantly smaller than that of the spherical model. Although a cokriging method is useful when a primary variable is undersampled and cross-correlated with a secondary variable, such as elevation, the degree of correlation between the primary and secondary variables did not solely determine the performance of the interpolation. The degree of spatial variations of the primary variable, air temperature in this case, significantly influenced the prediction errors of the method. As a result, RMSE changed seasonally, being low in the warm, dry season and high in the cool, wet season. This outcome clearly demonstrated that the accuracy of the multivariate cokriging method depends not only on a cross-correlation between the primary and secondary variables but also on the nature of local climate, which is more variable and storm-dominating in the cool season.

References

Barnes, W. L., Pagano, T. S., and Salomonson, V. V., 1998, Prelaunch characteristics of the Moderate Resolution Imaging Spectroradiometer (MODIS) in EOS-AM1, *IEEE Transactions on Geoscience and Remote Sensing*, 36, 1088-1100.

Barry, R. G. and Chorley, R. J., 1987, *Atmosphere, Weather and Climate*, Routledge, London.

Daly, C., Nelson, R. P., and Phillips, D. L., 1994, A statistical-topographic model for mapping climatological precipitation over mountainous terrain, *Journal of Applied Meteorology*, 33, 140-158.

Daly, C., Helmer, E. H., and Quiñones, M., 2003,

Mapping the climate of Puerto Rico, Vieques and Culebra, *International Journal of Climatology*, 23, 1359-1381.

Declercq, F. A. N., 1996, Interpolation methods for scattered sample data: accuracy, spatial patterns, processing time, *Cartography and Geographic Information Systems*, 23, 128-144.

Giambelluca, T. W. and Nullet, D., 1991, Influence of the trade-wind inversion on the climate of a leeward mountain slope in Hawaii, *Climate Research*, 1, 207-216.

Goovaerts, P., 2000, Geostatistical approaches for incorporating elevation into the spatial interpolation of rainfall, *Journal of Hydrology*, 228, 113-129.

Havesi, A. J., Flint, A. L., and Istok, J. D., 1992, Precipitation estimation in mountainous terrain using multivariate geostatistics. Part II: isohyetal maps, *Journal of Applied Meteorology*, 31, 677-688.

Ishida, T. and Kawashima, S., 1993, Use of cokriging to eastimate surface air temperature from elevation, *Theoretical and Applied Climatology*, 47, 147-157.

Issaks, E. H. and Srivastava, R. M., 1989, *An Introduction to Applied Geostatistics*, Oxford University Press, Oxford.

Jarvis, C. H., Stuart, N., and Cooper, W., 2003, Informetric and statistical diagnostics to provide artificially-intelligent support for spatial analysis: the example of interpolation, *International Journal of Geographical Information Science*, 17, 495-516.

Justice, D. H., Salomonsonm, V., Privette, J., Riggs, G., Strahler, A., Lucht, R., Myneni, R., Knjazihhin, Y., Running, S., Nemani, R., Vermte, E., Townsend, J., Dfries, R., Roy, D., Wan, Z., Huete, A., Leeuwen van, R., Wolfe, R., Giglio, L., Muller, J. P., Lewis, P., and Barnsley, M., 1998, The Moderate Resolution Imaging Spectroradiometer (MODIS): land remote sensing for global change research, *IEEE Transactions on Geoscience and Remote Sensing*, 36, 1228-1249.

Kaufman, Y. J., Herring, D. D., Ranson K. J., and Collatz, G. J., 1998, Earth observing system AM1 mission to earth, *IEEE Transactions on Geoscience and Remote Sensing*, 36, 1045-1055.

Lull, H. W. and Ellison, L., 1950, Precipitation in relation to altitude in central Utah, *Ecology*, 31, 479-484.

Martinez-Cob, A. and Cuenca, R. H., 1992, Influence of elevation on regional evapotranspiration using multivariate geostatistics for various climatic regimes in Oregon, *Journal of Hydrology*, 136, 353-380.

Martinez-Cob, A., 1996, Multivariate geostatistical analysis of evaportranspiration and precipitation in mountainous terrain, *Journal of Hydrology*, 174, 19-35.

Nullet, D., Juvik, J. O., and Wall, A., 1995, A Hawaiian mountain climate cross-section, *Climate Research*, 5, 131-137.

Nullet, D. and Sanderson, M., 1995, Radiation and energy balances and air temperature, in Sanderson, M. (eds.), *Prevailing Trade Winds-Weather and Climate in Hawaii*, University of Hawaii Press, Honolulu, 37-55.

Park, N. and Jang, D., 2008, Mapping of temperature and rainfall using DEM and multivariate kriging, *Journal of the Korean Geographical Society*, 43, 1002-1015

Phillips, D. L., Dolph, J., and Marks, D., 1992, A comparison of geostatistical procedures for spatial analysis of precipitation in mountainous terrain, *Agricultural and Forest Meteorology*, 58, 119-141.

Schroeder, T., 1995, Climate controls, in Sanderson, M. (ed.), *Prevailing Trade Winds-Weather and Climate in Hawaii*, University of Hawaii Press, Honolulu, 12-36.

Slocum, T. A., McMaster, R. B., Kessler, F. C., and Howard, H. H., 2009, *Thematic Cartography and Geovisualization*, Prentice Hall, Upper Saddle River, 286-287.

Vitousek, P. M., Aplet, G., and Turner, D., 1992, The Mauna Loa environmental matrix: foliar and soil nutrients, *Oecologia*, 89, 372-382.

Webster, R. and Oliver, M. A., 2001, *Geostatistics for Environmental Sciences*, Wiley, Chichester.

Zimmerman, D., Pavlik, C., Ruggles, A., and Armstrong, M. P., 1999, An experimental comparison of

ordinary and universal kriging and inverse distance weighting, *Mathematical Geology*, 31, 375-390.

Correspondence: Sunyurp Park, Department of Geography and Environmental Studies, University of Hawaii-Hilo, 200 W. Kawili Street, Hilo, Hawaii USA 96720 (e-mail: sunypark@hawaii.edu, phone: +1-808-974-7548)

교신: 박선엽, 하와이대학교-힐로, 지리학과, 200 W. Kawili Street, Hilo, Hawaii USA 96720 (이메일: sunypark@hawaii.edu, 전화: +1-808-974-7548)

Recieved March 21, 2009
Revised May 7, 2009
Accepted May 11, 2009